CMS Physics Analysis Summary

Contact: cms-pag-conveners-smp@cern.ch 2015/12/15

Measurement of the double-differential inclusive jet cross section at $\sqrt{s}$ = 13 TeV

The CMS Collaboration

Abstract

A measurement of the double-differential inclusive jet cross section, as a function of jet transverse momentum p_{T} and absolute jet rapidity $|y|$, is presented. The analysis is based on a data set of proton-proton collisions acquired by the CMS experiment at the LHC during 2015 at a center-of-mass energy of 13 TeV. The collected data correspond to an integrated luminosity of 72 pb^{-1} for rapidities up to $|y| = 3$ and 45 pb^{-1} for the forward rapidity region $3.2 < |y| < 4.7$. Jets are reconstructed with the anti-k_{T} clustering algorithm for two jet size parameters R=0.7 and R=0.4 in a phase space region covering jet p_{T} up to 2 TeV and jet rapidity up to $|y|$ = 4.7. The results are compared to fixed-order predictions of perturbative QCD and to simulations using various Monte Carlo event generators including parton showers, hadronisation, and multiparton interactions.

1 Introduction

The theory of Quantum Chromodynamics (QCD) is the fundamental underlying theory to describe interactions among quarks and gluons, i.e. partons. In QCD, partons are produced in hadron-hadron collisions with large cross sections. Experimentally, partons are resolved as jets. The inclusive jet production is one of the processes by which QCD can be tested in hadron colliders. Similar measurements have been carried out at the Large Hadron Collider (LHC) by the ATLAS and CMS collaborations at 2.76 TeV [1, 2], 7 TeV [3–6] and 8 TeV [7] center-of-mass energy as well as by experiments at other hadron colliders [8–12].

The measured inclusive jet cross section at $\sqrt{s}$ = 2.76, 7, and 8 TeV is in agreement within uncertainties with theoretical calculations at next-to-leading order (NLO) in the strong coupling α_S at small y, while bigger differences are observed at large y. The new energy regime provided by the so-called "LHC Run 2" at $\sqrt{s}$ = 13 TeV gives the opportunity to study and access a new kinematic region of momentum fraction x, where the parton density becomes large. Modifications to the parton evolution scheme may occur at small x, when the transverse momentum of the interacting partons cannot be neglected and a different parton evolution scheme might be more appropriate [13–15]. An investigation within the full rapidity range also allows to further investigate our understanding of the high and low x regime.

In this physics analysis summary, a measurement of the double-differential inclusive jet cross section, as a function of jet transverse momentum p_{T} and absolute jet rapidity $|y|$, is presented. The measurement is performed using data collected during 2015 by the CMS experiment at the LHC of proton-proton collisions at a center-of-mass energy $\sqrt{s}$ = 13 TeV. An integrated luminosity of 72 pb^{-1} is used for rapidities up to $|y| = 3$, while for the forward rapidity region $3.2 < |y| < 4.7$, 45 pb^{-1} are considered. The results are compared to fixed-order predictions of perturbative QCD (pQCD) and to simulations using various Monte Carlo (MC) event generators including the modeling of parton showers (PS), hadronization (HAD), and multiparton interactions (MPI).

2 Event selection and reconstruction

The measurement is based on data samples which are collected with single-jet high-level triggers (HLT) [16]. Eight such HLT single-jet triggers are considered, which are seeded by Level 1 (L1) triggers based on calorimetric information. They require, in the full rapidity coverage of the CMS detector, at least one jet with $p_{\mathrm{T}} > 60$, 80, 140, 200, 260, 300, 400, and 450 GeV in each event. Each of the considered triggers, except for the highest-threshold one, is prescaled during the first data taking period in 2015. The efficiency of each of the triggers is estimated by using lower-p_{T}-threshold triggers, and it is found to exceed 99% in the p_{T} regions used, shown in Table 1. The absolute efficiency scale is measured by using a single-jet trigger with p_{T} threshold equal to 40 GeV through the selection of a back-to-back dijet system matched to the HLT trigger objects, following the so-called "tag-and-probe" method; this trigger is found to have an efficiency larger than 99% for jet $p_{\mathrm{T}} > 80$ GeV.

The main physics objects are particle-flow (PF) [17, 18] jets reconstructed with the anti-k_{T} clustering algorithm, whose performance is discussed in [19]. The PF event algorithm reconstructs and identifies each individual particle by an optimized combination of information from the various subdetectors of the CMS detector. In this analysis are described measurements of jets clustered with two different values of the cone radius, R = 0.4 and R = 0.7, referred to as AK4 and AK7, respectively. In order to reduce the contribution of additional proton-proton interactions within the same beam crossing (pileup) to the reconstructed jets, the technique of charged

HLT path	p_T range (GeV)
PFJet_60	114-133
PFJet_80	133-220
PFJet_140	220-300
PFJet_200	300-430
PFJet_260	430-507
PFJet_300	507-638
PFJet_400	638-737
PFJet_450	> 737

Table 1: Trigger regions defined as ranges of the leading jet p_T in each event for every single jet trigger used in the inclusive jet cross section measurement.

hadron subtraction (CHS) [20] is considered. The presence of pileup results in unwanted calorimetric energy depositions and extra tracks. The CHS reduces these effects by removing tracks identified as originating from pileup vertices. The average number of pileup interactions observed for the considered data sample is about 21.

Reconstructed jets require small additional energy corrections to account for residual nonuniformities and nonlinearities in the detector response. Jet energy scale (JES) [21] corrections are derived using simulated events, generated by PYTHIA8 [22] with tune CUETM1[1] [23] and processed through the CMS detector simulation based on the GEANT 4 [24] package, and in situ measurements with dijet, photon+jet, and Z+jet events. An offset correction is applied to account for the extra energy clustered into jets due to additional pileup proton-proton interactions within the same or neighbouring bunch crossings. The JES correction, applied as a multiplicative factor to the four momentum jet vector, depends on the jet η and p_T values. For a jet with a p_T of 100 GeV the typical correction is about 10%, and decreases with increasing p_T.

Events are selected by requiring at least one good primary vertex (PV). A PV is required to be reconstructed from at least five charged particles measured in the tracker and to lie within 24 cm in the longitudinal direction with respect to the nominal interaction point and within 2 cm distance in the transverse plane with respect to the longitudinal direction. Jets are selected by starting from p_T = 114 GeV and grouped in seven different rapidity ($|y|$) bins: from $0 < |y| < 3.0$ in six steps of 0.5, while the last $|y|$ bin includes the region between 3.2 and 4.7 in absolute value of rapidity. Only jets with tight identification requirements are selected. These are based on different types of constituents inside the reconstructed jets and aim for rejection of non-physical jets arising from noise [25]. The efficiency of this set of identification criteria is greater than 99% for actual jets of hadrons.

3 Measurement of the double-differential inclusive jet cross section

The double-differential inclusive jet cross section is defined as

$$\frac{\mathrm{d}^2\sigma}{\mathrm{d}p_T\mathrm{d}y} = \frac{1}{\epsilon\mathcal{L}_{\mathrm{int,eff}}} \frac{\mathrm{N}_{\mathrm{jets}}}{\Delta p_T \cdot \Delta y} \,, \tag{1}$$

where ϵ is the product of the trigger and jet selection efficiencies, which is found to be greater

[1] The CUETM1 tune used for the PYTHIA8 MC event generator is sometimes referred to as CUETP8M1.

than 99%, $\mathcal{L}_{\text{int,eff}}$ is the integrated luminosity, N_{jets} is the number of jets in a bin with transverse momentum, Δp_T, and rapidity, Δy, widths. The phase space in rapidity is subdivided into six bins starting from $y = 0$ up to $|y| = 3$ with $|\Delta y| = 0.5$, plus one bin from $|y| = 3.2$ to $|y| = 4.7$ coresponding to the forward rapidity region.

The double-differential inclusive jet cross section is corrected for detector resolution effects and unfolded to the stable-particle level. In this way, a direct comparison of the measurement to results from other experiments and to QCD predictions is possible.

The unfolding procedure is based on the iterative d'Agostini method [26], as implemented in the ROOUNFOLD software package [27], using a response matrix that maps the physics distribution onto the measured one. The response matrix is derived from simulation, which uses as an input the theoretically predicted spectrum and introduces the smearing effects by taking into account the jet p_T resolution. The theoretically predicted spectrum is evaluated from fixed-order calculations based on the NLOJET++ program [28, 29], within the framework of the FASTNLO package [30] using the CT14 [31] parton distribution function (PDF) (more details are presented in the following sub-section 4.1). The jet p_T resolution is evaluated with the CMS detector simulation based on the PYTHIA8 event generator with tune CUETM1, after correcting for the residual differences with data [21]. The unfolding correction factors vary in average typically between 10 to 20%. Note that the statistical fluctuations observed in data before the unfolding might affect the statistical structure of neighboring bins after the unfolding, as well. However, it has been checked that the statistical uncertainty obtained after unfolding increases with respect to the measured data and the statistical structures in the unfolded spectra are always within the errors of the detector-level distributions.

The main systematic uncertainties arise in the jet measurements of both cone sizes from the estimation of the JES calibration, and the uncertainty of the integrated luminosity. The JES uncertainty, evaluated separately for AK4 and AK7 jets for the data recorded in 2015, is $\sim$1–3% in the central region ($|y| < 2$) and increases up to 7–8% in the forward rapidity region. The resulting uncertainties on the double-differential inclusive jet cross section range between 8% in the central rapidities and for low p_T to 65% for the outer rapidities and the highest p_T.

The uncertainty of the integrated luminosity propagates directly to the cross section and it is 4.8%.

The unfolding procedure is affected by uncertainties of the Jet Energy Resolution (JER) parametrization. Alternative response matrices, which are built by varying the JER pararameters by one standard deviation up and down [21], are used to unfold the measured spectra. The JER uncertainty introduces a 1-2% uncertainty on the cross section. The model dependence of the theoretical p_T spectrum also affects the response matrix and thus the unfolding, but this uncertainty has negligible effects on the cross section measurement.

Finally, an uncertainty of 1% on the cross section measurement is assigned to account for residual effects of small inefficiencies from jet identification from both online and offline. The total experimental systematic uncertainty on the measured cross section is obtained by summing in quadrature the single contributions from JES, luminosity, JER, and jet identification uncertainties.

4 Theory predictions

4.1 Predictions from fixed-order calculations in pQCD

The theoretical predictions for the jet cross section are known at NLO accuracy in pQCD and are evaluated by using the NLOJET++ program version 4.1.13 [28, 29], within the framework of FASTNLO programm version 2.3.1 [30]. The cross sections are calculated at NLO for single inclusive jet production. The renormalisation and the factorisation scale (μ_r and μ_f) are chosen to be equal to the jet p_{T}. The number of the quarks that are assumed to be massless in the calculation is set to five. The calculation is performed using four different PDF sets with NLO evolution: CT14 [31], HERAPDF1.5 [32], MMHT2014 [33], and NNPDF3.0 [34] with the default values of the strong coupling $\alpha_S(M_Z) = 0.1180$, 0.1176, 0.1200, and 0.1180, respectively.

The theoretical uncertainties are the quadratic sum of the scale, PDF, and α_S uncertainties. The scale uncertainty is calculated by varying the renormalisation and the factorisation scales to the following six combinations: ($\mu_r/\ p_{\mathrm{T}}$, $\mu_f/\ p_{\mathrm{T}}$) = (0.5,0.5), (0.5,1), (1,0.5), (1,2), (2,1) and (2,2). The maximum upwards and downwards deviation from the cross section calculated using ($\mu_r/\ p_{\mathrm{T}}$, $\mu_f/\ p_{\mathrm{T}}$) = (1,1) is considered as the uncertainty. The PDF and α_S uncertainties are calculated according to the prescription of CT14 at 90% confidence level, scaled down to 68.3% confidence level.

The impact of non-perturbative (NP) effects, i.e. MPI and HAD effects, are evaluated by using samples obtained from different MC event generators with a simulation of parton-shower and underlying-event (UE) contributions. The leading order (LO), PYTHIA 8 [22] with tune CUETM1 [23] and HERWIG ++ [35] with tune UE-EE-5C [36] and CUETS1 [23], and the NLO, POWHEG [37–39], MC event generators are considered for the estimation of the NP corrections. The matrix-element calculation performed with POWHEG is interfaced to PYTHIA 8 with three different tunes (CUETS1-CTEQ6L1, CUETS1-HERAPDF and CUETM1 [23]) for the UE simulation. The cross section ratios between a nominal event generation interfaced to the simulation of underlying-event contributions and a sample without hadronization and MPI effects are taken as correction separately in each considered rapidity range. In a compact formulation, the NP correction factors can be defined as:

$$C^{\mathrm{NP}} = \frac{\frac{d\sigma^{\mathrm{PS+HAD+MPI}}}{dp_{\mathrm{T}}}}{\frac{d\sigma^{\mathrm{PS}}}{dp_{\mathrm{T}}}} \tag{2}$$

where $\sigma^{\mathrm{PS+HAD+MPI}}$ is the cross section obtained with a MC sample simulating the contribution of PS, HAD and MPI, while σ^{PS} includes only PS effects. Corrections obtained with various NLO and LO event generators are evaluated separately for AK7 and AK4 jets. The average of results from NLO and LO event generators has been considered as central value of the NP corrections and fitted to a power-law function. The uncertainty carried by the NP corrections has been evaluated by fitting the envelopes of the predictions of the different generators used. The combinations of PDF, matrix element and tunes used for the evaluation of the NP corrections have been validated on UE, Minimum Bias (MB) and jet variables and they are able to reproduce a wide set of observables [23]. In Fig. 1 and 2, NP corrections are shown, respectively, for AK7 and AK4 jets in two rapidity bins, an inner ($0.5< |y| < 1.0$) and an outer ($2.5< |y| < 3.0$) one.

The NP corrections for AK7 jets are observed to be of the order of 15% (13%) for $p_{\mathrm{T}} \sim 100$ GeV in $0.5 < |y| < 1.0$ ($2.5 < |y| < 3.0$) and decrease rapidly for increasing p_{T}, flattening at values of 1 for $p_{\mathrm{T}} \sim 200$–300 GeV, depending on the considered rapidity range. Due to the smaller cone sizes, AK4 jets are less affected by MPI and hadronization effects. In particular, the

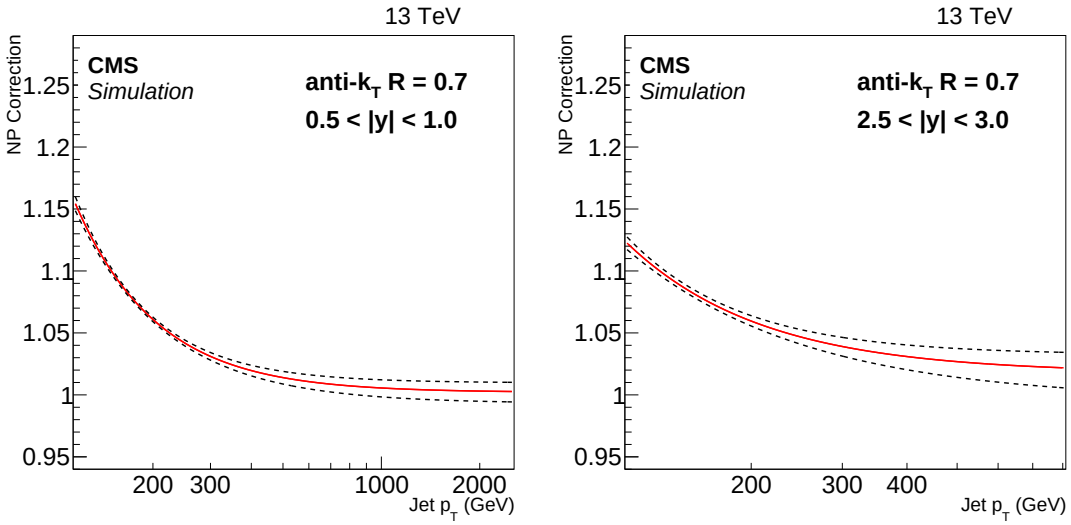

Figure 1: Fits to the nonperturbative corrections obtained for inclusive AK7 jet cross sections as a function of jet p_{T} for two rapidity bins: $0.5 < |y| < 1.0$ (left) and $2.5 < |y| < 3.0$ (right).

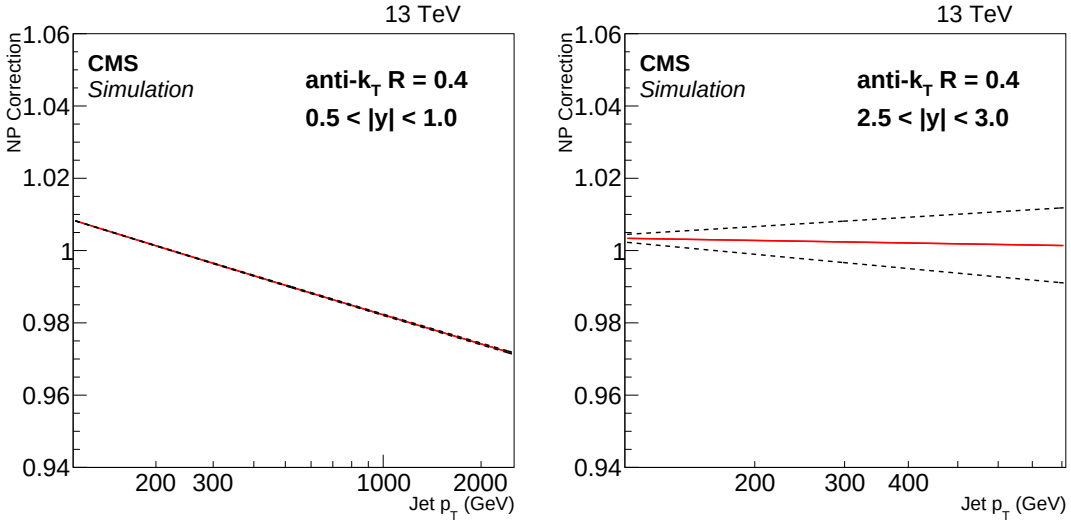

Figure 2: Fits to the nonperturbative corrections obtained for inclusive AK4 jet cross sections as a function of jet p_{T} for two rapidity bins: $0.5 < |y| < 1.0$ (left) and $2.5 < |y| < 3.0$ (right).

additional energy produced by MPI shrinks for decreasing R values while out-of-cone losses due to hadronization effects increase for smaller R. These two effects are responsible for NP corrections which go below 1 for $p_{\mathrm{T}} > 200$ GeV at central rapidities, observed for AK4 jets. However, the NP corrections are very close to 1 in the whole considered phase space. For both cone sizes, the uncertainty assigned to the NP corrections is of the order of 1–2%.

Electroweak effects, which arise from virtual exchange of massive gauge W and Z bosons, may become sizeable at high jet p_{T} and central rapidity. For jet measurements performed at center-of-mass energies of 7 [40] and 8 [7] TeV, electroweak corrections are observed of $\sim$ 10–15% for jet $p_{\mathrm{T}} > 1$ TeV in $|y| < 1.0$, decreasing below 2% for lower p_{T} independently of the jet rapidity. In the phase space measured for this analysis, the electroweak effects are not found to be relevant because of the large statistical uncertainties affecting the measurement at high jet p_{T}. Hence, no electroweak corrections are applied to the predicted hard-scattering cross section at the current stage.

4.2 Predictions from fixed-order calculations matched to parton shower simulations

Predictions from different Monte Carlo (MC) event generators are also compared to data. The HERWIG ++ (version 2.7.0) [35] and the PYTHIA 8.204 [22] event generators are considered. Both of them are based on a LO 2$\rightarrow$2 matrix element calculation. The PYTHIA 8 event generators simulates parton showers ordered in transverse momentum and use the Lund string model [41] for hadronization, while HERWIG ++ generates parton showers through angular-ordered emissions and uses a cluster fragmentation model [42] for hadronization. The contribution of MPI is simulated in PYTHIA 8 and HERWIG ++. In particular, the PYTHIA 8 event generator applies a model [43] where MPI are interleaved with parton showering, while HERWIG ++ models the overlap between the colliding protons by means of the Fourier transform of the electromagnetic form factor, which plays the role of an effective inverse proton radius. Depending on the amount of proton overlap, the contribution of generated MPI varies in the simulation. For both PYTHIA and HERWIG ++, the free parameters related to the MPI simulation are obtained from tunes to measurements in pp collision at the LHC, while the parameters used for hadronization are determined from fits to LEP data for both PYTHIA [43] and HERWIG [44]. For PYTHIA 8, the CUETM1 tune [23] is considered, while predictions from the HERWIG ++ event generator are obtained with the, CUETS1 tune [23]. The former tune is based on the NNPDF2.3LO [45, 46] PDF set, while the CTEQ6L1 PDF set [47] is used in the latter one.

Predictions based on NLO pQCD are also considered from calculations using the POWHEG package [37–39] matched to PYTHIA parton showers and including a simulation of MPI. The POWHEG sample uses the CT10nlo PDF set [48]. Various tunes in PYTHIA 8 are used for the UE simulation which differ in the choice of the PDF set and the hadronization parameters: the CUETM1 tune [23], determined with the NNPDF2.3LO PDF set [45, 46], and tunes CUETS1-CTEQL1 and CUETS1-HERAPDF [23], which use the CTEQ6L1 [47] and the HERAPDF1.5LO [49] PDF sets respectively. The hadronization parameters for the CUETM1 tune are taken from the Monash tune, while the 4C tune provides them for both CUETS1 tunes. All these combinations of POWHEG matrix element and UE-simulation tunes reproduce with very high precision UE and jet observables at various collision energies [23].

5 Comparison of theory and data

Figure 3 shows the double-differential inclusive jet cross section measurement, presented as a function of p_{T} in the considered $|y|$ ranges, after unfolding for detector effects. Jets are clustered

with the anti-k_T algorithm considering R = 0.7. On the left, the measurement is compared to NLOJET++ predictions based on the CT14 PDF set corrected for NP effects. On the right, the measurement is compared to predictions from POWHEG + PYTHIA8 with tune CUETM1. Figure 4 shows the double-differential jet cross section for the jet cone radius R = 0.4. The data are consistent with the predictions for a wide range of jet p_T from 114 GeV up to 2 TeV.

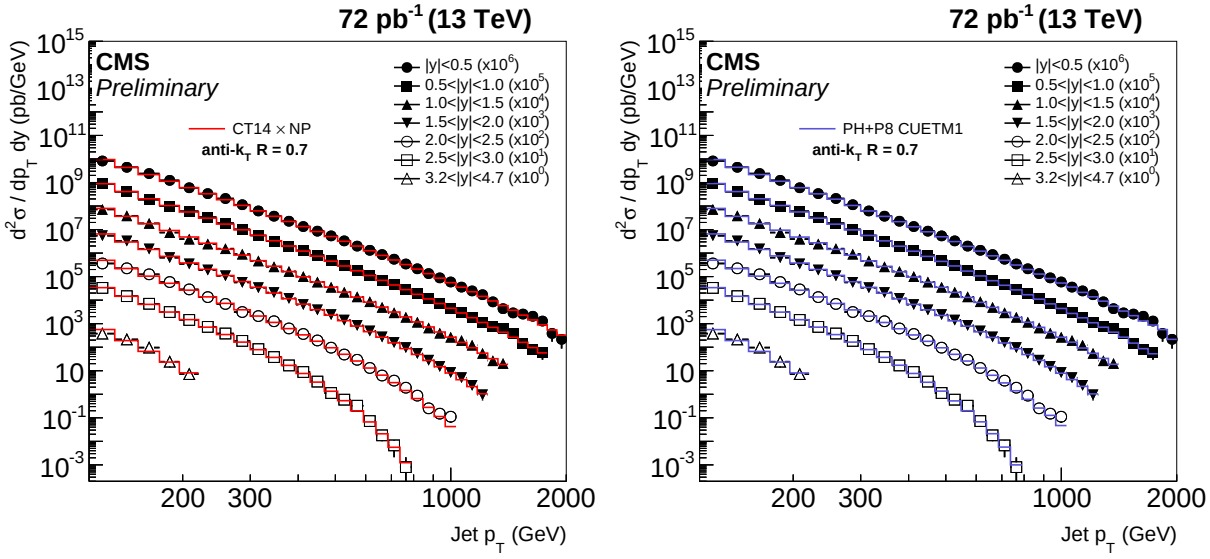

Figure 3: Double-differential inclusive jet cross section as function of jet p_T. On the left, data (points) and NLOJet++ predictions based on CT14 PDF set corrected for the NP factor (line). On the right, data (points) and predictions from POWHEG + PYTHIA8 with tune CUETM1 (line). Jets are clustered with the anti-k_T algorithm (R = 0.7).

The ratios of data over the NLOJET++ predictions using the CT14 PDF set are shown in Fig. 5 for radius R = 0.7. The error bars on the points correspond to the statistical uncertainty and the shaded band to the total experimental systematic uncertainty. For comparison, predictions employing three other alternative PDF sets are also shown. Figure 6 shows the results for the small radius R = 0.4. An overall good level of agreement within uncertainties is observed between data and predictions in the whole studied kinematic range for both jet cone sizes. However, for R = 0.4, the data are systematically overestimated by about 5–10%, while a better description is provided for jets reconstructed with R = 0.7. This is due to PS and soft-gluon resummation contributions which are missing in fixed-order calculations and are more relevant for smaller jet cone sizes.

The ratios of data over predictions from POWHEG + PYTHIA8 with tune CUETM1 are shown in Fig. 7 for radius R = 0.7. Likewise, the error bars on the points correspond to the statistical uncertainty and the shaded band to the total experimental systematic uncertainty. For comparison, predictions employing four other MC event generators are also shown. Figure 8 shows the results for the small radius R = 0.4. There is an overall good level of agreement within uncertainties in the whole studied kinematic range between data and predictions from POWHEG + PYTHIA8 with various tunes. The agreement of data with the PYTHIA8 predictions is very poor, while for HERWIG++ significant disagreements are observed.

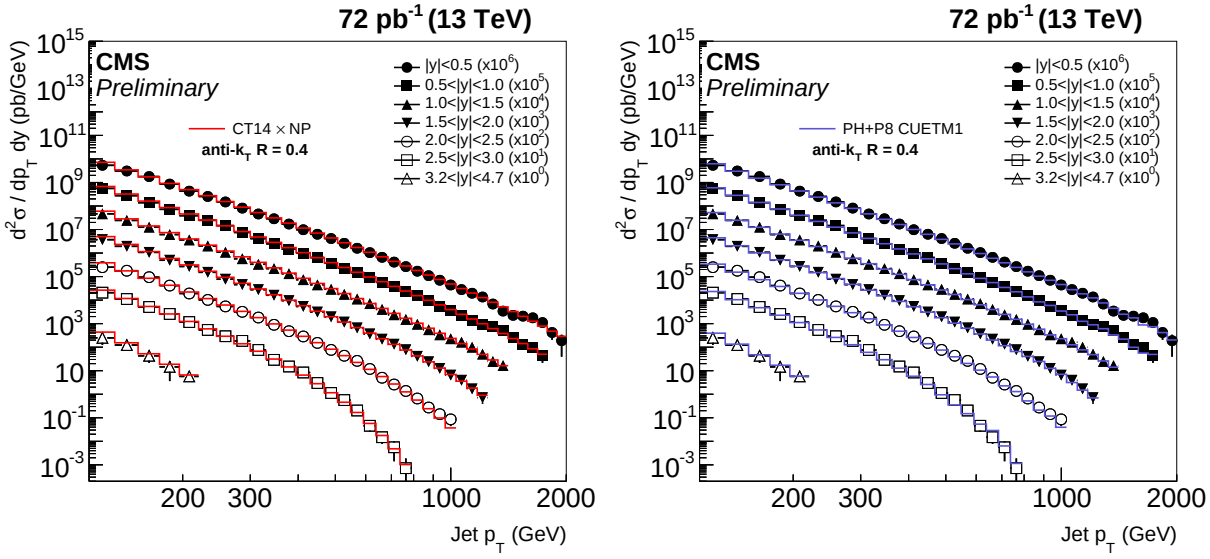

Figure 4: Double-differential inclusive jet cross section as function of jet p_{T}. On the left, data (points) and NLOJet++ predictions based on CT14 PDF set corrected for the NP factor (line). On the right, data (points) and predictions from POWHEG + PYTHIA8 with tune CUETM1 (line). Jets are clustered with the anti-k_{T} algorithm (R = 0.4).

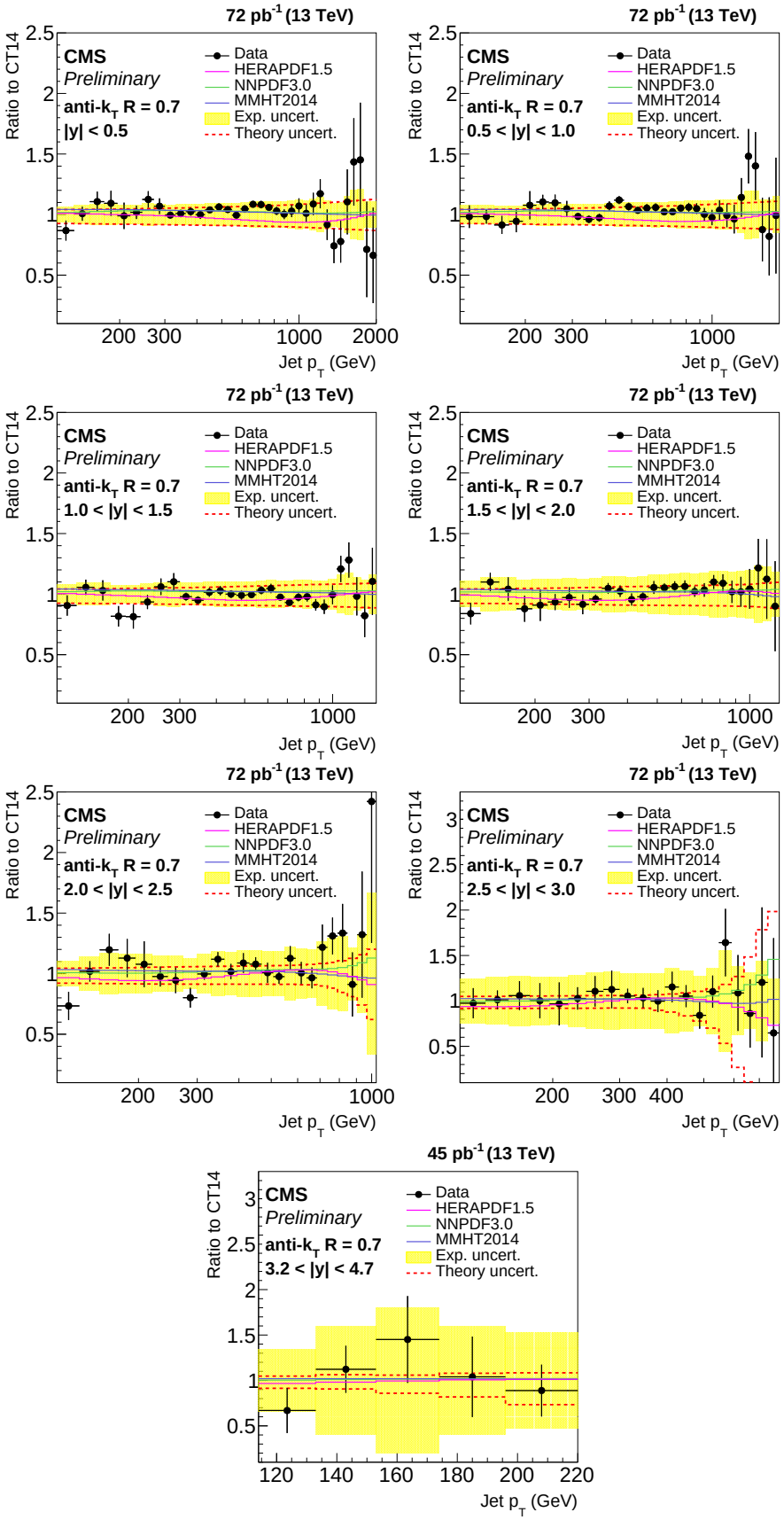

Figure 5: Ratio of data over theory prediction using the CT14 PDF set. For comparison predictions employing three other PDF sets are also shown. Jets are clustered with the anti-k_T algorithm (R = 0.7). The error bars correspond to the statistical uncertainty of the data and the shaded band to the total systematical uncertainty.

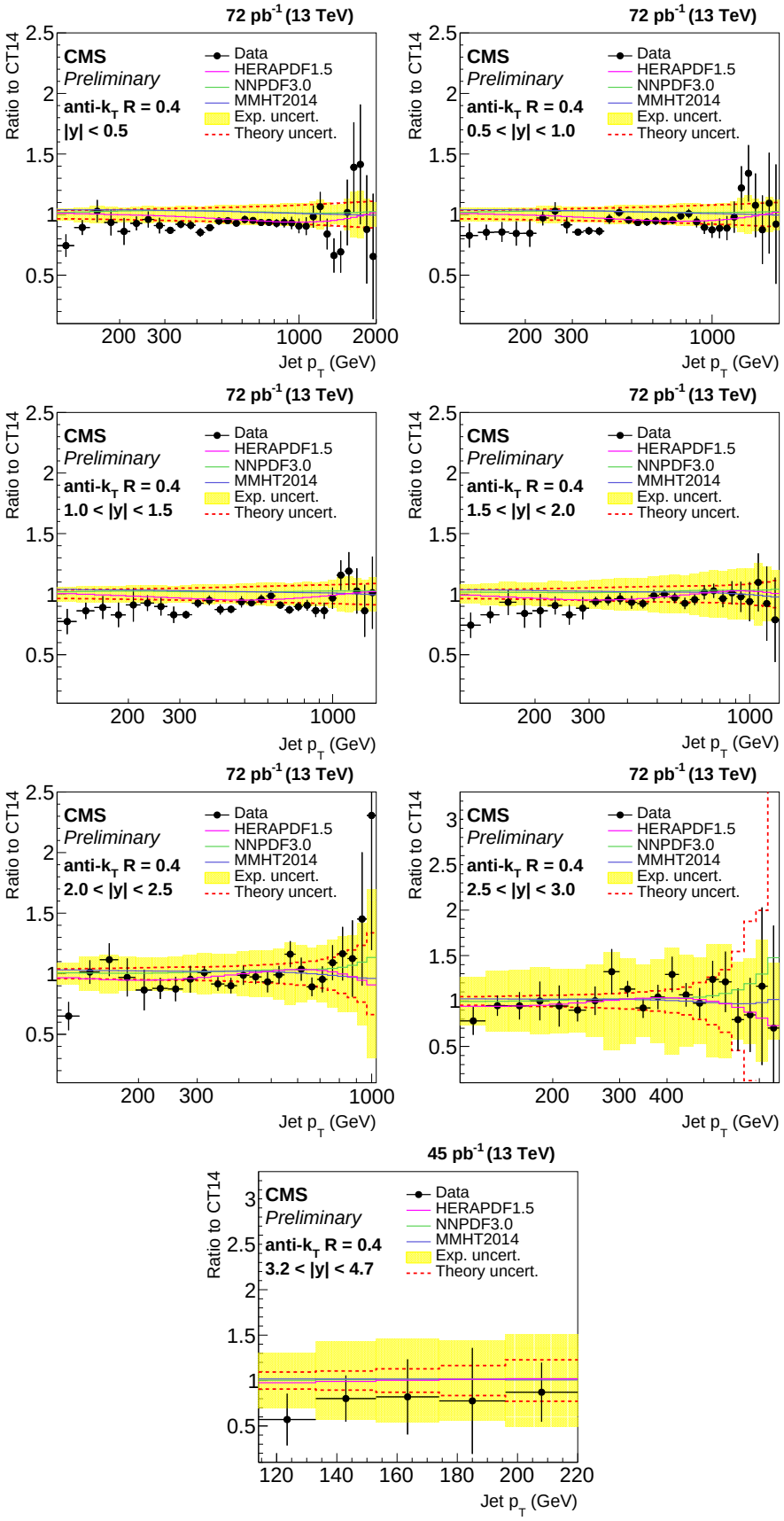

Figure 6: Ratio of data over theory prediction using the CT14 PDF set. For comparison predictions employing three other PDF sets are also shown. Jets are clustered with the anti-k_T algorithm (R = 0.4). The error bars correspond to the statistical uncertainty of the data and the shaded band to the total systematical uncertainty.

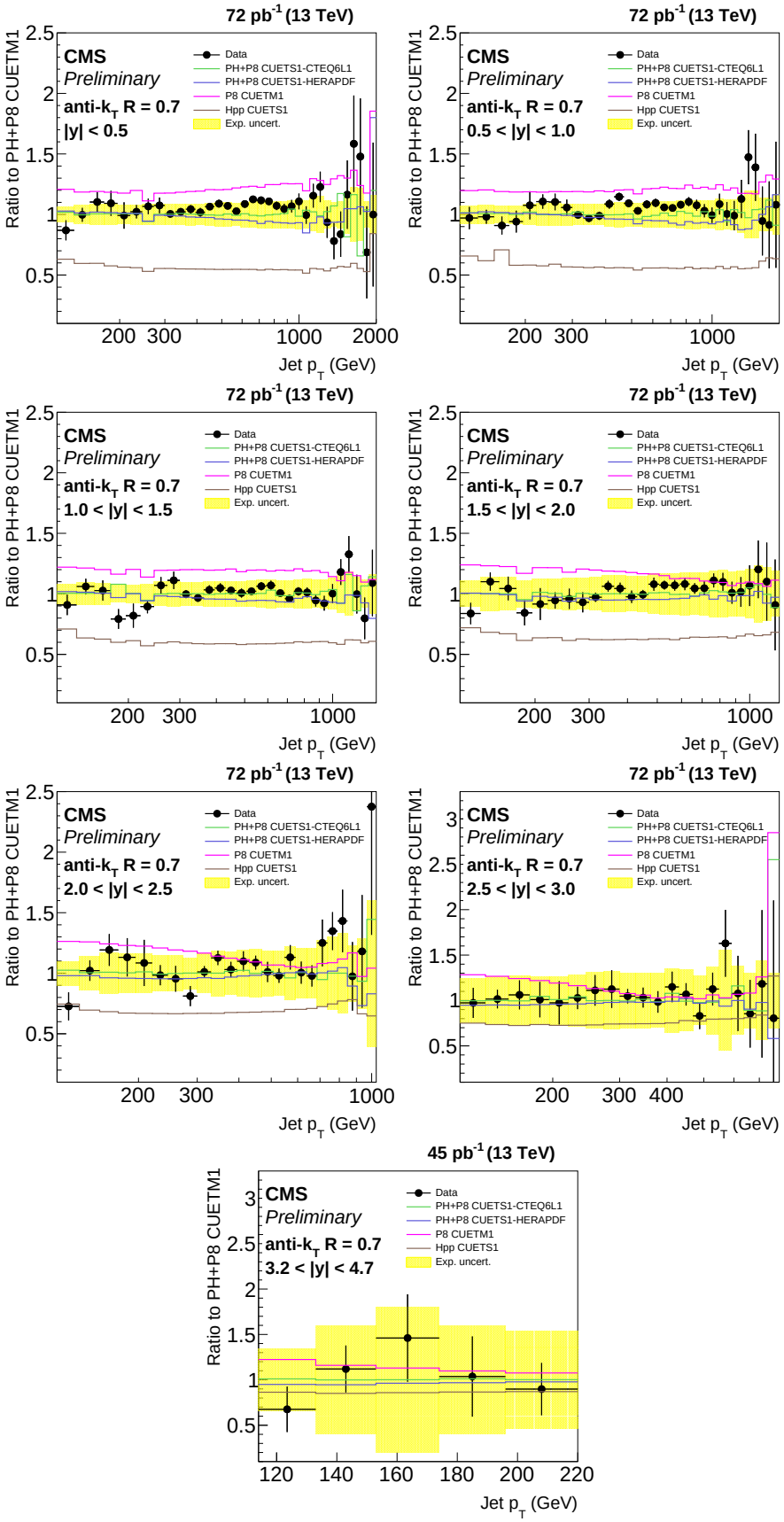

Figure 7: Ratio of data over predictions from POWHEG + PYTHIA8 with tune CUETM1. For comparison predictions employing four other MC generators are also shown, where PH, P8 and Hpp stands for POWHEG, PYTHIA8 and HERWIG ++ respectively. Jets are clustered with the anti-k_T algorithm (R = 0.7). The error bars correspond to the statistical uncertainty of the data and the shaded band to the total systematical uncertainty.

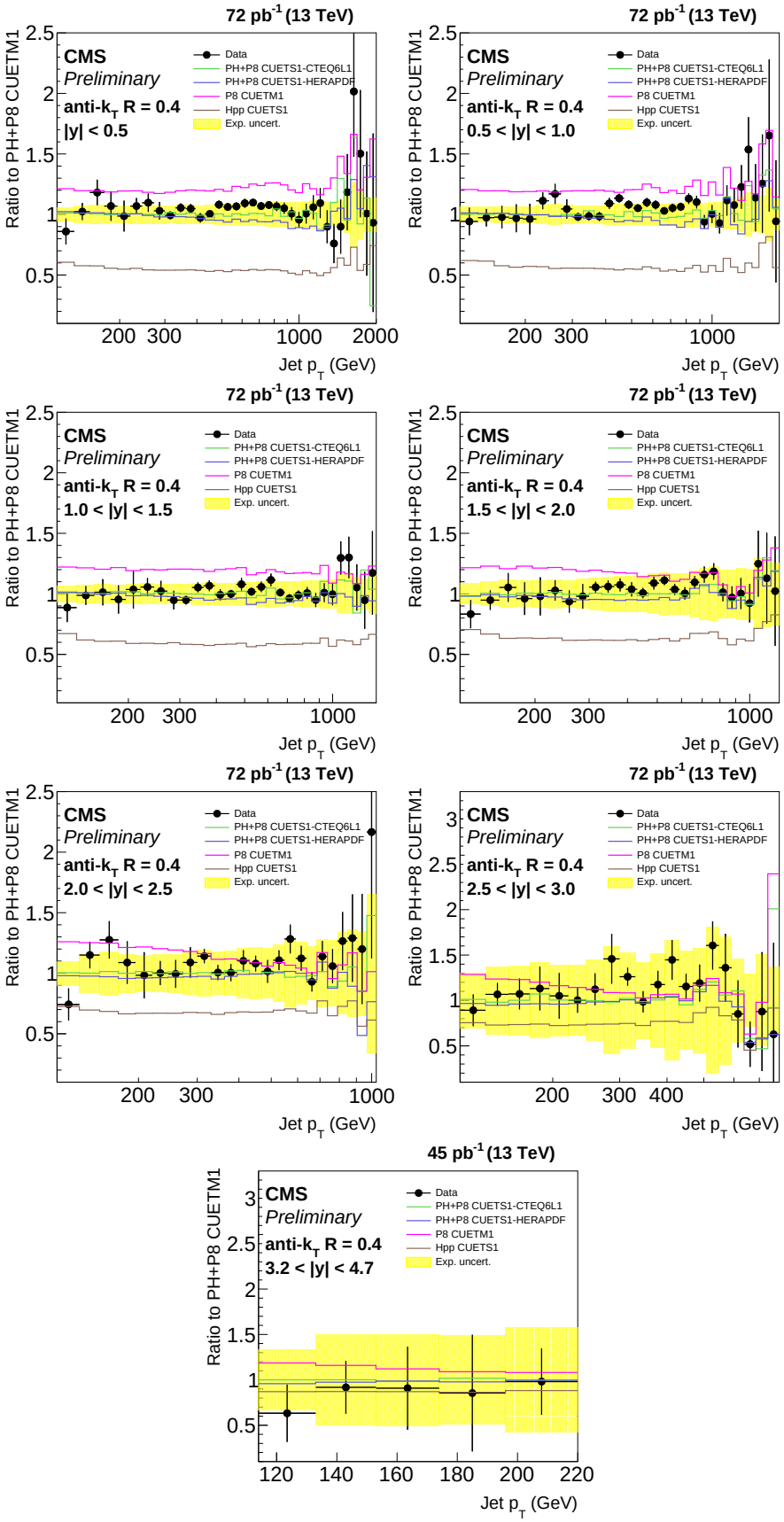

Figure 8: Ratio of data over predictions from POWHEG + PYTHIA8 with tune CUETM1. For comparison predictions employing four other MC generators are also shown, where PH, P8 and Hpp stands for POWHEG, PYTHIA8 and HERWIG ++ respectively. Jets are clustered with the anti-k_T algorithm (R = 0.4). The error bars correspond to the statistical uncertainty of the data and the shaded band to the total systematical uncertainty.

6 Summary

A measurement of the inclusive jet cross section, as a function of jet transverse momentum p_T and absolute rapidity $|y|$, is presented using data from proton-proton collisions at $\sqrt{s} = 13$ TeV collected with the CMS detector. The result covers a large range in jet p_T from 114 GeV up to 2 TeV, in six rapidity bins starting from $|y| = 0$ up to $|y| = 3$ with $|\Delta y| = 0.5$, and one bin from $|y| = 3.2$ to $|y| = 4.7$ corresponding to the forward rapidity region. The measurement has been performed for two different jet cone radii R = 0.4 and 0.7 for the anti-k_T jet algorithm. Data corresponding to an integrated luminosity of 72 pb^{-1} for rapidities up to $|y| = 3$ and of 45 pb^{-1} for the forward rapidity region have been analyzed.

By comparing the data to predictions at NLO accuracy in pQCD, it is observed that jet cross sections for the larger jet size of R = 0.7 are better described than for R = 0.4. In contrast, NLO predictions matched to parton showers from POWHEG + PYTHIA8, even with two different tunes, perform equally well for both jet size parameters as the fixed-order prediction for the larger jet size of R = 0.7. This is in agreement with the meassurement performed at the center-of-mass energy of 7 TeV [50], where it was observed that POWHEG + PYTHIA8 correctly describes the R dependence of the inclusive jet cross section, while fixed-order predictions at NLO fail in that respect.

Predictions by the LO MC generators PYTHIA8 and HERWIG++ exhibit significant discrepancies with respect to data. The discrepancies are more pronounced in the case of HERWIG++ .

References

[1] ATLAS Collaboration, "Measurement of the inclusive jet cross-section in pp collisions at $\sqrt{s} = 2.76$ TeV and comparison to the inclusive jet cross-section at $\sqrt{s} = 7$ TeV using the ATLAS detector", *Eur. Phys. J. C* **73** (2013) 2509, doi:10.1140/epjc/s10052-013-2509-4, arXiv:1304.4739.

[2] CMS Collaboration, "Measurements of the inclusive jet cross section in pp collisions at $\sqrt{s} = 2.76$ TeV", CMS Physics Analysis Summary CMS-SMP-14-017, 2015.

[3] ATLAS Collaboration, "Measurement of inclusive jet and dijet cross sections in proton-proton collisions at 7 TeV centre-of-mass energy with the ATLAS detector", *Eur. Phys. J. C* **71** (2011) 1512, doi:10.1140/epjc/s10052-010-1512-2, arXiv:1009.5908.

[4] CMS Collaboration, "Measurement of the Inclusive Jet Cross Section in pp Collisions at 7 TeV", *Phys. Rev. Lett.* **107** (2011) 132001, doi:10.1103/PhysRevLett.107.132001, arXiv:1106.0208.

[5] ATLAS Collaboration, "Measurement of inclusive jet and dijet production in pp collisions at $\sqrt{s} = 7$ TeV using the ATLAS detector", *Phys. Rev. D* **86** (2012) 014022, doi:10.1103/PhysRevD.86.014022, arXiv:1112.6297.

[6] CMS Collaboration, "Measurements of differential jet cross sections in proton-proton collisions at $\sqrt{s} = 7$ TeV with the CMS detector", *Phys. Rev. D* **87** (2013), no. 11, 112002, doi:10.1103/PhysRevD.87.112002, arXiv:1212.6660.

[7] CMS Collaboration, "Measurements of the double-differential inclusive jet cross section in pp collisions at $\sqrt{s} = 8$ TeV", CMS Physics Analysis Summary CMS-SMP-14-001, 2015.

[8] UA2 Collaboration, "Observation of Very Large Transverse Momentum Jets at the CERN $\bar{p}p$ Collider", *Phys. Lett. B* **118** (1982) 203, doi:10.1016/0370-2693(82)90629-3.

[9] UA1 Collaboration, "Hadronic Jet Production at the CERN Proton-Antiproton Collider", *Phys. Lett. B* **132** (1983) 214, doi:10.1016/0370-2693(83)90254-X.

[10] CDF Collaboration, "Measurement of the Inclusive Jet Cross Section using the k_T algorithm in $p\bar{p}$ Collisions at $\sqrt{s}$ = 1.96 TeV with the CDF II Detector", *Phys. Rev. D* **75** (2007) 092006, doi:10.1103/PhysRevD.75.119901,10.1103/PhysRevD.75.092006, arXiv:hep-ex/0701051.

[11] D0 Collaboration, "Measurement of the inclusive jet cross-section in $p\bar{p}$ collisions at $\sqrt{s}$ = 1.96 TeV", *Phys. Rev. Lett.* **101** (2008) 062001, doi:10.1103/PhysRevLett.101.062001,arXiv:0802.2400.

[12] CDF Collaboration, "Measurement of the Inclusive Jet Cross Section at the Fermilab Tevatron $p\bar{p}$ Collider Using a Cone-Based Jet Algorithm", *Phys. Rev. D* **78** (2008) 052006, doi:10.1103/PhysRevD.79.119902,10.1103/PhysRevD.78.052006, arXiv:0807.2204.

[13] M. Ciafaloni, D. Colferai, and G. P. Salam, "Renormalization group improved small x equation", *Phys. Rev.* **D60** (1999) 114036, doi:10.1103/PhysRevD.60.114036, arXiv:hep-ph/9905566.

[14] S. J. Brodsky et al., "The QCD pomeron with optimal renormalization", *JETP Lett.* **70** (1999) 155–160, doi:10.1134/1.568145,arXiv:hep-ph/9901229.

[15] V. S. Fadin and L. N. Lipatov, "BFKL pomeron in the next-to-leading approximation", *Phys. Lett.* **B429** (1998) 127–134, doi:10.1016/S0370-2693(98)00473-0, arXiv:hep-ph/9802290.

[16] CMS Collaboration, "The CMS High Level Trigger", *Eur. Phys. J. C* **46** (2006) 605, doi:10.1140/epjc/s2006-02495-8,arXiv:hep-ex/0512077.

[17] CMS Collaboration, "Commissioning of the Particle-flow Event Reconstruction with the first LHC collisions recorded in the CMS detector", CMS Physics Analysis Summary CMS-PFT-10-001, 2010.

[18] CMS Collaboration, "Particle-Flow Event Reconstruction in CMS and Performance for Jets, Taus, and MET", CMS Physics Analysis Summary CMS-PFT-09-001, 2009.

[19] M. Cacciari, G. P. Salam, and G. Soyez, "The Anti-k(t) jet clustering algorithm", *JHEP* **04** (2008) 063, doi:10.1088/1126-6708/2008/04/063,arXiv:0802.1189.

[20] CMS Collaboration, "Jet Energy Corrections and Uncertainties. Detector Performance Plots for 2012.", Technical Report CMS-DP-2012-012, 2012.

[21] CMS Collaboration, "Determination of Jet Energy Calibration and Transverse Momentum Resolution in CMS", *JINST* **6** (2011) P11002, doi:10.1088/1748-0221/6/11/P11002,arXiv:1107.4277.

[22] T. Sjostrand, S. Mrenna, and P. Z. Skands, "A Brief Introduction to PYTHIA 8.1", *Comput. Phys. Commun.* **178** (2008) 852–867, doi:10.1016/j.cpc.2008.01.036, arXiv:0710.3820.

[23] CMS Collaboration, "Event generator tunes obtained from underlying event and multiparton scattering measurements", (2015). arXiv:1512.00815.

[24] GEANT4 Collaboration, "Geant4–a simulation tool kit", *Nucl. Instrum. Meth. A* **506** (2003) 250, doi:10.1016/S0168-9002(03)01368-8.

[25] CMS Collaboration, "Calorimeter Jet Quality Criteria for the First CMS Collision Data", CMS Physics Analysis Summary CMS-JME-09-008, 2010.

[26] G. D'Agostini, "A Multidimensional unfolding method based on Bayes' theorem", *Nucl. Instrum. Meth. A* **362** (1995) 487, doi:10.1016/0168-9002(95)00274-X.

[27] T. Adye, "Unfolding algorithms and tests using RooUnfold", 2011. arXiv:1105.1160. doi:10.5170/CERN-2011-006.

[28] Z. Nagy, "Three-jet cross sections in hadron-hadron collisions at next-to-leading order", *Phys. Rev. Lett.* **88** (2002) 122003, doi:10.1103/PhysRevLett.88.122003, arXiv:hep-ph/0110315.

[29] Z. Nagy, "Next-to-leading order calculation of three-jet observables in hadron-hadron collisions", *Phys. Rev. D* **68** (2003) 094002, doi:10.1103/PhysRevD.68.094002, arXiv:hep-ph/0307268.

[30] D. Britzger, K. Rabbertz, F. Stober, and M. Wobisch, "New features in version 2 of the fastNLO project", doi:10.3204/DESY-PROC-2012-02/165, arXiv:1208.3641.

[31] S. Dulat et al., "The CT14 Global Analysis of Quantum Chromodynamics", (2015). arXiv:1506.07443.

[32] ZEUS, H1 Collaboration, "Combined Measurement and QCD Analysis of the Inclusive e+- p Scattering Cross Sections at HERA", *JHEP* **01** (2010) 109, doi:10.1007/JHEP01(2010)109, arXiv:0911.0884.

[33] L. A. Harland-Lang, A. D. Martin, P. Motylinski, and R. S. Thorne, "Parton distributions in the LHC era: MMHT 2014 PDFs", *Eur. Phys. J.* **C75** (2015), no. 5, 204, doi:10.1140/epjc/s10052-015-3397-6, arXiv:1412.3989.

[34] NNPDF Collaboration, "Parton distributions for the LHC Run II", *JHEP* **04** (2015) 040, doi:10.1007/JHEP04(2015)040, arXiv:1410.8849.

[35] J. Bellm et al., "Herwig++ 2.7 Release Note", (2013). arXiv:1310.6877.

[36] M. H. Seymour and A. Siodmok, "Constraining MPI models using σ_{eff} and recent Tevatron and LHC Underlying Event data", *JHEP* **10** (2013) 113, doi:10.1007/JHEP10(2013)113, arXiv:1307.5015.

[37] P. Nason, "A New method for combining NLO QCD with shower Monte Carlo algorithms", *JHEP* **11** (2004) 040, doi:10.1088/1126-6708/2004/11/040, arXiv:hep-ph/0409146.

[38] S. Frixione, P. Nason, and C. Oleari, "Matching NLO QCD computations with Parton Shower simulations: the POWHEG method", *JHEP* **11** (2007) 070, doi:10.1088/1126-6708/2007/11/070, arXiv:0709.2092.

[39] S. Alioli et al., "Jet pair production in POWHEG", *JHEP* **04** (2011) 081, doi:10.1007/JHEP04(2011)081, arXiv:1012.3380.

[40] CMS Collaboration, "Constraints on parton distribution functions and extraction of the strong coupling constant from the inclusive jet cross section in pp collisions at $\sqrt{s} = 7$ TeV", *Eur. Phys. J.* **C75** (2015), no. 6, 288, doi:10.1140/epjc/s10052-015-3499-1, arXiv:1410.6765.

[41] B. Andersson, "The Lund model", *Camb. Monogr. Part. Phys. Nucl. Phys. Cosmol.* **7** (1997).

[42] B. R. Webber, "A QCD Model for Jet Fragmentation Including Soft Gluon Interference", *Nucl. Phys.* **B238** (1984) 492, doi:10.1016/0550-3213(84)90333-X.

[43] R. Corke and T. Sjostrand, "Interleaved Parton Showers and Tuning Prospects", *JHEP* **03** (2011) 032, doi:10.1007/JHEP03(2011)032, arXiv:1011.1759.

[44] S. Gieseke et al., "Herwig++ 2.5 Release Note", (2011). arXiv:1102.1672.

[45] NNPDF Collaboration, "Parton distributions with QED corrections", *Nucl. Phys.* **B877** (2013) 290–320, doi:10.1016/j.nuclphysb.2013.10.010, arXiv:1308.0598.

[46] NNPDF Collaboration, "Unbiased global determination of parton distributions and their uncertainties at NNLO and at LO", *Nucl. Phys.* **B855** (2012) 153–221, doi:10.1016/j.nuclphysb.2011.09.024, arXiv:1107.2652.

[47] J. Pumplin et al., "New generation of parton distributions with uncertainties from global QCD analysis", *JHEP* **07** (2002) 012, doi:10.1088/1126-6708/2002/07/012, arXiv:hep-ph/0201195.

[48] H.-L. Lai et al., "New parton distributions for collider physics", *Phys. Rev.* **D82** (2010) 074024, doi:10.1103/PhysRevD.82.074024, arXiv:1007.2241.

[49] A. M. Cooper-Sarkar, "HERAPDF1.5LO PDF Set with Experimental Uncertainties", *PoS* **DIS2014** (2014) 032.

[50] CMS Collaboration, "Measurement of the ratio of inclusive jet cross sections using the anti-k_T algorithm with radius parameters $R = 0.5$ and 0.7 in pp collisions at $\sqrt{s} = 7$ TeV", *Phys. Rev. D* **90** (2014) 072006, doi:10.1103/PhysRevD.90.072006, arXiv:1406.0324.